

of the $\text{Mo}_6\text{Cl}_{8-n}\text{S}_n$ series with high-sulfide contents can be similarly prepared, providing incentive for work currently under way aimed at synthesizing discrete Mo_6S_8 cluster derivatives.

The substitution of a single chloride by sulfide dramatically alters the electronic structure of the Mo_6X_8 cluster. One indicator of the change in electronic structure is the change in color going from $\text{Mo}_6\text{Cl}_8^{4+}$ (yellow) to $\text{Mo}_6\text{Cl}_7\text{S}^{3+}$ (red). Another indicator is the decreased difference between the XPS binding energies of the bridging and terminal chlorides in $\text{Mo}_6\text{Cl}_7\text{S}^{3+}$ (1.8 eV) in comparison to $\text{Mo}_6\text{Cl}_8^{4+}$ (2.2 eV).

In contrast to the differences evident in the electronic structure, the Mo-Mo and Mo-Cl bond distances in $\text{Mo}_6\text{Cl}_7\text{S}^{3+}$ are nearly identical with those of $\text{Mo}_6\text{Cl}_8^{4+}$. However, subtle differences in bond lengths in the structure

of $(\text{pyH})_3[(\text{Mo}_6\text{Cl}_7\text{S})\text{Cl}_6]$ permit the crystallographic sites occupied by the bridging sulfide to be located.

Acknowledgment. We thank the National Science Foundation for a grant to the Department of Chemistry for the purchase of the photoelectron spectrometer used in this research.

Registry No. $(\text{pyH})_3[(\text{Mo}_6\text{Cl}_7\text{S})\text{Cl}_6]$, 75085-32-4; $(\text{pyH})_3[(\text{Mo}_6\text{Cl}_7\text{S})\text{Cl}_6]\cdot 3\text{pyHCl}$, 75069-92-0; $\text{Mo}_6\text{Cl}_{12}$, 11062-51-4; $[(n\text{-C}_4\text{H}_9)_4\text{N}]_2[(\text{Mo}_6\text{Cl}_8)\text{Cl}_6]$, 12367-12-3; $(\text{pyH})_2[(\text{Mo}_6\text{Cl}_8)\text{Cl}_6]$, 80754-08-1.

Supplementary Material Available: Listings of structure factor amplitudes, anisotropic temperature factors, and C-C or C-N bond distances (26 pages). Ordering information is given on any current masthead page.

Contribution from the Institut für Physikalische und Theoretische Chemie der Universität Tübingen, 7400 Tübingen, West Germany, and the Anorganisch-Chemisches Institut der Universität Göttingen, 3400 Göttingen, West Germany

Gas-Phase Molecular Structure of Sulfur Tetrafluoride Methylimide, $\text{CH}_3\text{N}=\text{SF}_4$. An NMR, Electron Diffraction, Microwave, and ab Initio Study

HORST GÜNTHER, HEINZ OBERHAMMER,* RÜDIGER MEWS, and INGO STAHL

Received July 14, 1981

The molecular structure of $\text{CH}_3\text{N}=\text{SF}_4$ in the gas phase has been determined by joint analysis of electron diffraction and microwave spectroscopy data. A strongly distorted trigonal-bipyramidal structure with the double bond in equatorial position and the methyl group pointing in axial direction has been obtained, confirming the interpretation of the NMR spectra. Geometric parameters are compared to the ab initio results for $\text{HN}=\text{SF}_4$, and the bond angles around the sulfur atom are correlated with the electronic structure of the $\text{S}=\text{N}$ π bond. The temperature dependence of the NMR spectra is discussed.

Introduction

Molecular structures and bonding properties of penta-coordinate sulfur(VI) compounds are particularly interesting. For a long time $\text{O}=\text{SF}_4^2$ was the only known member in this class of molecules. Only recently the "isoelectronic" sulfur tetrafluoride imides $\text{RN}=\text{SF}_4^{3-6}$ and methylene sulfur tetrafluoride $\text{CH}_2=\text{SF}_4^7$ were synthesized. Whereas $\text{O}=\text{SF}_4^8$ and $\text{CH}_2=\text{SF}_4^{9,10}$ have been studied in greater detail, only little is known about the various sulfur tetrafluoride imides.¹¹ In this study we report the NMR spectra and gas-phase structure investigation for $\text{CH}_3\text{N}=\text{SF}_4$. For this molecule only the combination of electron diffraction data and rotational constants allows a reliable structure determination without constraints for the bond distances. A structure determination from electron diffraction data alone would require serious geometric constraints due to the high correlations between various bond distances.

Experimental Section

CH_3NSF_4 was prepared according to the literature method.⁵ It was separated from impurities (CH_3F , NSF_3) by fractional condensation (-120 , -196 °C) under vacuum. The pure compound (checked by IR and NMR spectroscopy) remained in the -120 °C trap. The compound is very sensitive to moisture; it readily hydrolyses to give CH_3NSOF_2 and CH_3NHSF_5 . NMR spectra were recorded with a Bruker E 60, ^{19}F NMR spectra with a Bruker WH 360 FT (at the University of Bremen), and ^1H spectra also with a Varian XL 200 (at the Institute for Organic Chemistry, University of Göttingen).

The electron diffraction intensities were recorded with a Balzers diffractograph KD-G2¹² at two camera distances, 50 and 25 cm. Details of the experiment are listed in Table I. (Throughout this

Table I. Details of Electron Diffraction Experiment

camera dist, cm	50	25
nozzle diameter, mm	0.2	0.2
sample temp, °C	-40	-42
nozzle temp, °C	10	10
camera pressure, torr	2×10^{-5}	10^{-5}
exposure time, s	8-25	25-60
electron wavelength, Å	0.048 87 (1)	0.048 85 (1)
s range, Å ⁻¹ α	1.6-17	10-35

$\alpha = (4\pi/\lambda) \sin(\theta/2)$. λ = electron wavelength; θ = scattering angle.

Table II. Rotational Constants (GHz) for $\text{CH}_3\text{N}=\text{SF}_4$

	A	B	C
B_0^i	3.34307 (3)	2.14935 (1)	1.87452 (1)
B_z^i	3.34126 (28)	2.14865 (11)	1.87380 (11)
$B_z^i(\text{calcd})$	3.34144	2.14871	1.87384

paper 1 Å = 100 pm, 1 torr = 101.325/760 kPa, and 1 cal = 4.184 J.) The electron wavelength was determined by ZnO powder dif-

- (1) Preliminary geometric parameters, based on electron diffraction data only, have been cited by O. Glemser and R. Mews, *Angew. Chem.*, **92**, 904 (1980); *Angew. Chem., Int. Ed. Engl.*, **19**, 883 (1980).
- (2) O. Ruff and H. Jones, *Naturforsch. Med. Deutschland 1939-44*, **23**, 182; H. Jones, *Z. Anorg. Allg. Chem.*, **265**, 273 (1951).
- (3) C. W. Tullock, D. D. Coffman, and E. L. Muetterties, *J. Am. Chem. Soc.*, **86**, 357 (1964).
- (4) (a) I. Stahl, R. Mews, and O. Glemser, *J. Fluorine Chem.*, **7**, 55 (1976); (b) *Angew. Chem.*, **92**, 393 (1980); *Angew. Chem., Int. Ed. Engl.*, **19**, 408 (1980).
- (5) R. Mews, *Angew. Chem.*, **90**, 561 (1978); *Angew. Chem., Int. Ed. Engl.*, **17**, 530 (1978).
- (6) D. D. Des Marteau and K. Seppelt, *Angew. Chem.*, **92**, 659 (1980); *Angew. Chem., Int. Ed. Engl.*, **19**, 643 (1980).
- (7) G. Kleemann and K. Seppelt, *Angew. Chem.*, **90**, 547 (1978); *Angew. Chem., Int. Ed. Engl.*, **17**, 516 (1978).

* To whom correspondence should be addressed at the Institut für Physikalische und Theoretische Chemie der Universität Tübingen.

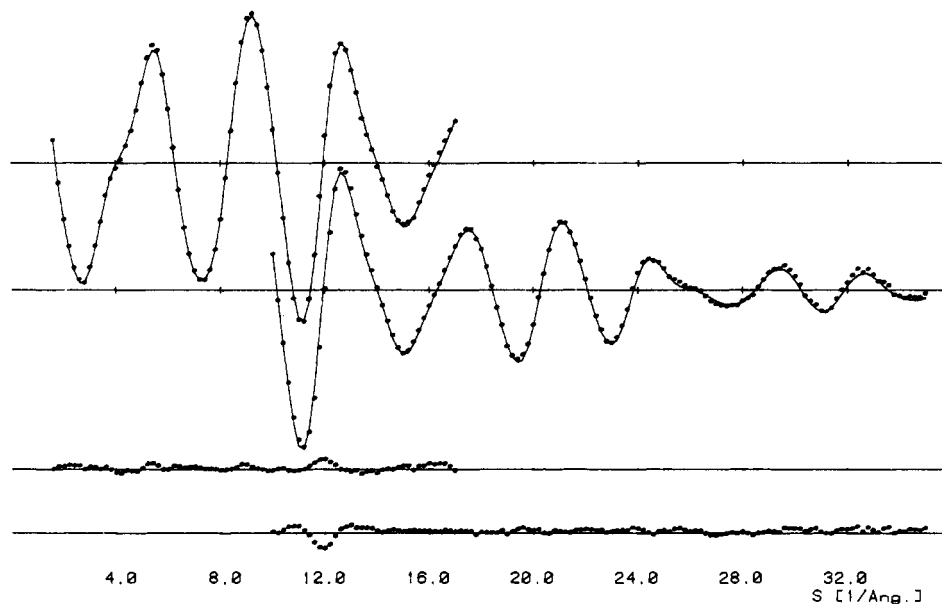


Figure 1. Experimental (O) and calculated (—) molecular intensities and differences.

Table III. Geometric Parameters for CH₃N=SF₄, FN=SF₄, and HN=SF₄ in Å and Deg (Atom Numbering in Figure 2)

	CH ₃ N=SF ₄ ^a	FN=SF ₄ ^b	HN=SF ₄ ^c
S=N	1.480 (6)	1.520 (9)	1.461
S-F _e	1.567 (4)	1.564 (5)	1.550
S-F _a	1.643 (4)	1.615 (7)	1.611
S-F _a '	1.546 (7)	1.535 (12)	1.569
N-X ^d	1.441 (16)	1.357 (8)	1.003
F _e SF _e	102.6 (0.2)	99.8 (0.3)	104.9
NSF _a	98.4 (0.4)	96.9 (0.4)	96.9
NSF _a '	94.6 (0.4)	90.6 (0.5)	96.8
F _a SF _a '	167.0 (0.6)	172.5 (0.7)	166.3
SNX	127.2 (1.1)	117.6 (1.2)	117.8

^a Electron diffraction and microwave data (r_{α}° structure) of this study. ^b Electron diffraction and microwave data (r_{α}° structure) of ref 19. ^c Ab initio calculations (r_e structure) of this study. ^d X = C, F, or H.

fraction. Two plates for each camera distance were selected and evaluated by the usual procedure.¹³ Numerical values for the total scattering intensities in steps of $\Delta s = 0.2 \text{ \AA}^{-1}$ of the two sets of plates are deposited as supplementary data.¹⁴ The averaged molecular intensities are presented in Figure 1.

The microwave spectra were recorded with a conventional Stark spectrometer¹⁵ in the range 8–39 GHz. The Stark field varied between 100 and 1600 V cm⁻¹. R-branch transitions for $J = 1$ to $J = 9$ and Q-branch transitions for $J = 12$ to $J = 37$ were measured and assigned. Due to a low barrier to internal rotation of the methyl group most transitions are split into A and E components. Rotational and centrifugal distortion constants for both species were determined by least-squares analysis. The rotational constants corrected for internal rotation effects are listed in Table II.¹⁶ Error limits for B_0^i ($B^i =$

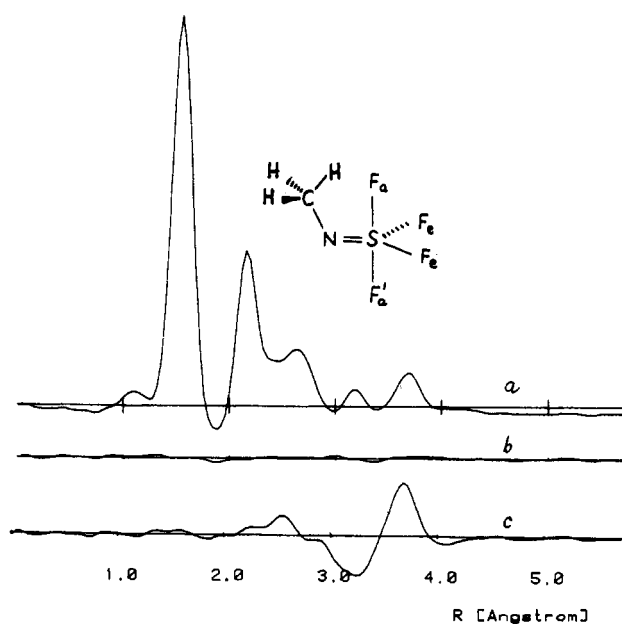


Figure 2. Experimental radial distribution function (curve a), difference curve for methyl group in axial plane (curve b), and difference curve for methyl group in equatorial plane (curve c).

A, B, C) are standard deviations.

Structure Analysis

A preliminary geometric model was derived from the experimental radial distribution function (Figure 2). Satisfactory agreement between experimental and calculated radial distribution functions is obtained only for models with the methyl group in axial position, i.e., in the axial plane of the SF₄ group (see Figure 2). The effect of the position of the methyl group relative to the SF₄ group on the radial distribution function is demonstrated in Figure 2. Curve b shows the difference between experiment and final models (geometric parameters of Table III) with the axial position of the CH₃ group, and c is the difference curve of a refined model with the CH₃ group constrained to the equatorial plane. The preliminary geometric parameters and some vibrational am-

- (8) G. Gundersen and K. H. Hedberg, *J. Chem. Phys.*, **51**, 2500 (1969).
- (9) H. Bock, J. E. Boggs, G. Kleemann, D. Lentz, H. Oberhammer, E. M. Peters, K. Seppelt, A. Simon, and B. Solouki, *Angew. Chem.*, **91**, 1008 (1979); *Angew. Chem., Int. Ed. Engl.* **18**, 944 (1979).
- (10) H. Oberhammer and J. E. Boggs, *J. Mol. Struct.*, **56**, 107 (1979).
- (11) From NMR investigations it was concluded that RNSF₄ compounds should have a *tbp* structure with R in an axial position: E. L. Muetterties, W. Mahler, K. Packer, and R. Schmutzler, *Inorg. Chem.*, **3**, 1298 (1964).
- (12) H. Oberhammer in "Molecular Structure by Diffraction Methods", Vol. 4, G. A. Sim and L. E. Sutton, Ed., The Chemical Society, Burlington House, London, 1976.
- (13) H. Oberhammer, W. Gombler, and H. Willner, *J. Mol. Struct.*, **70**, 273 (1981).
- (14) Supplementary data.
- (15) H. D. Kamphusmann, Ph.D. Thesis, Universität Ulm, 1970.

- (16) Details of the microwave study have been reported at the V. European Microwave Conference, Tübingen, West Germany, 1980, and will be published elsewhere.

Table IV. Vibrational Amplitudes from Electron Diffraction (ED) and Spectroscopic Data (spec) and Harmonic Vibrational Corrections (without Distances Involving Hydrogen Atoms)^a

	ED	spec	$r_a - r_\alpha^\circ$
S=N	0.040 ^b	0.040	0.0007
S-F _e	0.043 ^b	0.043	0.0016
S-F _{a'}	0.044 ^b	0.044	0.0006
S-F _{a''}	0.043 ^b	0.043	0.0005
N-C	0.047 ^b	0.047	0.0059
F _e ···F _e	0.074 ^b	0.074	0.0005
F _e ···F _{a'}	} 0.062 (5)	0.066	0.0011
F _e ···F _{a''}		0.062	0.0006
N···F _e		0.058	0.0012
N···F _{a'}		0.053 ^b	0.0005
N···F _{a''}		0.053 ^b	0.0013
F _{a'} ···F _{a''}	0.052 ^b	0.052	0.0002
S···C	0.074 (20)	0.063	0.0010
F _e ···C	0.081 (23)	0.094	-0.0014
F _{a'} ···C	0.106 ^b	0.106	-0.0014
F _{a''} ···C	0.066 ^b	0.066	0.0002

^a For atom numbering, see Figure 2. Error limits are 3 σ values.^b Value not refined.

plitudes were then refined by a joint least-squares procedure based on the molecular intensities and rotational constants.¹⁷ The harmonic vibrational corrections for the rotational constants, $\Delta B^i = B_o^i - B_z^i$, and for the interatomic distances, $\Delta r = r_a - r_\alpha^\circ$, were calculated with the program NORCOR¹⁸ from an approximate force field. For the N=SF₄ entity, the force constants for FN-SF₄¹⁹ were transferred. Standard values for the N-CH₃ entity were used. The torsional force constant for the CH₃ group was derived from the barrier to internal rotation which was determined to be 1150 \pm 50 cal mol⁻¹ from the microwave analysis. The anharmonicity constant was set to $a = 2 \text{ \AA}^{-1}$ for bonded distances and $a = 0$ for nonbonded distances. The corrected rotational constants B_z^i are listed in Table II, and the corrections Δr and parallel vibrational amplitudes are summarized in Table IV. Error limits for the B_z^i constants are increased by the uncertainties in the corrections ΔB^i , which are estimated to be 15% of the corrections. This uncertainty should include errors due to the small amplitude approximation used in these calculations. Molecular intensities are calculated with the scattering amplitudes and phases of ref 20, and a diagonal weight matrix was applied to the intensities.¹³ The relative weight of electron diffraction and microwave data were adjusted until the rotational constants were reproduced within their estimated error limits ($W_{MW,ED} = 250^{17b}$).

In the structure determination, the S=N bond was assumed to be coplanar with the equatorial plane of SF₄ group. Least-squares refinements with starting values of $\pm 5^\circ$ for this out of plane angle converged toward planarity within the estimated uncertainty. The C-H bond lengths and HCH angles were fixed at 1.09 \AA and 109 $^\circ$, respectively. Vibrational amplitudes for all bonded and some nonbonded distances (see Table IV) were fixed at their spectroscopic values. The effect of these constraints on the geometric parameters was studied by varying the vibrational amplitudes for the bonded distances systematically by $\pm 0.004 \text{ \AA}$. Assuming the CH₃ group to eclipse the S=N bond results in a slightly smaller sum of the errors squared (by 9%) than the staggered position. The results of the joint least-squares analysis are summarized in Tables III (geometric parameters) and IV (vibrational amplitudes).

Table V. Atomic Net Charges and Bond Overlap Populations (in au) for HN=SF₄^c

Atomic Net Charges			
S	2.188+	F _{a'}	0.450-
F _e	0.386-	N	0.845-
F _{a''}	0.493-	H	0.372+
Overlap Populations			
S-F _e	0.190 (0.065)	S=N	σ 0.110 (0.041)
S-F _{a'}	0.161 (0.058)		π_{e_a} 0.207 (0.035)
S-F _{a''}	0.188 (0.064)		π_{a_b} 0.100 (0.021)
		total	0.417 (0.097)

^a π -Bond density in equatorial plane. ^b π -Bond density in axial plane. ^c The contributions involving S(3d) functions are given in parentheses.

The estimated uncertainties for the geometric parameters are based on 2 σ values and include systematic errors due to the constraint of the bonded vibrational amplitudes. The agreement factors for the molecular intensities are $R_{50} = 3.8\%$ and $R_{25} = 7.6\%$ for the two camera distances. The calculated rotational constants are listed in Table II.

Ab Initio Calculations. So that the effort of ab initio calculations could be reduced, calculations with full geometry optimization for HN=SF₄ were performed with the ab initio gradient program TEXAS.²¹ The 21 and 4-21²² basis sets were used for hydrogen and second-row elements, respectively. For sulfur, the 3-3-21 basis sets derived by Skancke et al.²³ were supplemented by d functions which are constructed from slightly displaced p functions²² with an orbital exponent $\eta = 0.8$. Previous calculations for SF₄, O=SF₄, and H₂C=SF₄¹⁰ demonstrated that experimental molecular geometries are reproduced very well with these basis sets, with the sulfur d functions, however, being very important.

The optimized geometric parameters for HN=SF₄ are listed in Table III together with the experimental values for CH₃-N=SF₄ (these will be discussed below). Analogous to the position of the methyl group in CH₃N=SF₄, the energetically favored position of the hydrogen atom in HN=SF₄ is in the axial plane. When the hydrogen atom is rotated in the equatorial plane, the total energy increases by 25 kcal mol⁻¹. In this calculation the optimized geometric parameters for the axial configuration were used. Attempts to optimize the geometry of the equatorial configuration failed since this conformation does not represent an energy minimum. Ab initio calculations for X=SF₄ molecules¹⁰ (X = O or CH₂) demonstrated that the bond angles in the SF₄ group can be correlated with the charge distribution in the S=X π bond. Thereby, high π -electron density in the equatorial plane decreases the F_eSF_e angle (this is observed in H₂C=SF₄), and high π -electron density in the axial plane decreases the F_aSF_a angle (this is observed in O=SF₄) and vice versa.

The results of a Mulliken population analysis²⁴ are summarized in Table V. The atomic net charges indicate a very high polarity of the S=N bond that is even higher than for the S=O bond in thionyl tetrafluoride.¹⁰ The "shape" of the S=N π bond, i.e., the charge densities in the equatorial and axial plane, is intermediate between the S=O and S=C bonds in O=SF₄ and H₂C=SF₄. This π -bond charge distribution correlates qualitatively very well with the axial and equatorial FSF bond angles, which are also intermediate between the corresponding angles in O=SF₄ and H₂C=SF₄.

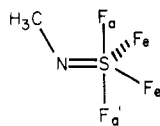
NMR Spectra. At room temperature the ¹H NMR spectrum consists of a quintet, and the ¹⁹F spectrum shows a broad

- (17) (a) K. Kuchitsu, *Gas Electron Diffraction*, *MTP Int. Rev. Sci.: Phys. Chem., Ser. One*, **2** (1972). (b) V. Typke, M. Dakkouri, and H. Oberhammer, *J. Mol. Struct.*, **44**, 85 (1978).
 (18) D. Christen, *J. Mol. Struct.*, **48**, 101 (1978).
 (19) D. D. Des Marteau, H. Eysel, H. Günther, and H. Oberhammer, *Inorg. Chem.*, in press.
 (20) J. Haase, *Z. Naturforsch., A*, **25A**, 936 (1970).

- (21) P. Pulay, *Theor. Chim. Acta*, **50**, 299 (1979).
 (22) P. Pulay, G. Fogarasi, and J. E. Boggs, *J. Am. Chem. Soc.*, **101**, 2550 (1979).
 (23) P. N. Skancke, G. Fogarasi, and J. E. Boggs, *J. Mol. Struct.*, **62**, 259 (1980).
 (24) R. S. Mulliken, *J. Chem. Phys.*, **23**, 1833 (1955).

singlet (Δ 100 Hz), suggesting equivalence of all sulfur-bonded fluorine atoms. At higher temperatures the ^{19}F signal becomes narrower (Δ at 80 °C 12 Hz), but no fine structure is observed due to the line broadening by the nitrogen.

Spectroscopic equivalence of the fluorine atoms is removed at low temperatures. As observed with sulfur tetrafluoride perfluoroalkylimides,^{11,4b} a complex pattern arises which has the general appearance of an ABC_2X_3 spectrum (at -60 °C).



$$\begin{aligned} \delta_{\text{F}_a} & 76.30, \delta_{\text{F}_a'} & 73.86, \delta_{\text{F}_e} & 68.25 \\ \delta_{\text{H}} & 2.89 \\ J_{\text{F}_a-\text{F}_a'} & 29.3, J_{\text{F}_a-\text{F}_e} & 194, J_{\text{F}_a-\text{H}} & 1.8 \\ J_{\text{F}_a'-\text{F}_e} & 201, J_{\text{F}_a'-\text{H}} & 0.5, J_{\text{F}_e-\text{H}^+} & -6.7 \end{aligned}$$

The coalescence temperature is difficult to determine; it is estimated at about -30 °C. Below -60 °C the spectra do not change. In *tbp* molecules, the chemical shifts for equatorial fluorine atoms are expected at higher field strengths than for the axial.¹¹ Therefore these data suggest that the F_e are equivalent. According to the polarity rule,²⁵ the third equatorial position should be occupied by the nitrogen. The axial fluorines will only be nonequivalent when the methyl group is axial.

Discussion

Table III compares experimental geometric parameters for $\text{CH}_3\text{N}=\text{SF}_4$ and $\text{FN}=\text{SF}_4$ and *ab initio* results for $\text{HN}=\text{SF}_4$. For a trigonal bipyramid the VSEPR model²⁶ predicts the axial bonds to be longer than the equatorial bonds. Among other examples this is confirmed by the experimental results for distorted trigonal bipyramids with C_{2v} symmetry such as SF_4 ,²⁷ $\text{O}=\text{SF}_4$,⁸ and $\text{CH}_2=\text{SF}_4$.⁹ It is also true for the average values of the two axial bonds in the sulfur tetrafluoride imides where the symmetry is reduced to C_s . In $\text{CH}_3\text{N}=\text{SF}_4$ and $\text{FN}=\text{SF}_4$, however, the axial bonds in direction of the nitrogen lone pairs ($\text{S}-\text{F}_a'$) are considerably shorter (by 0.097 and 0.080 Å, respectively) than the axial bonds in direction of the nitrogen substituent ($\text{S}-\text{F}_a$). The former bonds are even shorter than the equatorial bonds. This difference between the two axial bond lengths is not as pronounced in the *ab initio* result for $\text{HN}=\text{SF}_4$ (0.042 Å), and here both axial bonds are longer than the equatorial bonds. The effect of the nitrogen sub-

stituent on the distortion of the C_{2v} symmetry of the SF_4 group is also reflected in the difference between the NSF_a and NSF_a' angles. This difference is negligible in $\text{HN}=\text{SF}_4$ and increases with methyl or fluorine substitution. If the methyl group eclipses the $\text{S}=\text{N}$ bond—this configuration is slightly preferred by the structure analysis—one $\text{H}\cdots\text{F}_a$ interatomic distance is only about 2.00 Å. This small $\text{H}\cdots\text{F}$ distance and the relatively high internal rotation and pseudorotation barriers may be evidence for internal hydrogen bonding. On the other hand, the large $\text{N}=\text{S}-\text{F}_a$ (98.4°) and $\text{S}=\text{N}-\text{C}$ angles (127.2°, i.e., about 10° larger than the $\text{S}=\text{N}-\text{F}$ angle in $\text{FN}=\text{SF}_4$) probably result from unfavorable crowding in the resulting “five-membered ring”. In trigonal-bipyramidal molecules such as $\text{X}=\text{SF}_4$ ($\text{X} = \text{O}$ or CH_2), the bond angles around the sulfur atom strongly depend on the “shape” of the $\text{S}=\text{X}$ double bond.^{10,28} As pointed out above, this effect can be rationalized qualitatively by different populations of the π -bond orbitals in equatorial and axial direction. On the basis of this correlation between the F_eSF_e angle and the population of the equatorial π -bond orbital, we expect increasing π -bond charge density in the equatorial plane in the sequence $\text{O}=\text{SF}_4$ ($\text{F}_e\text{SF}_e = 114.9^\circ$) < $\text{CH}_3\text{N}=\text{SF}_4$ ($\text{F}_e\text{SF}_e = 102.6^\circ$) < $\text{FN}=\text{SF}_4$ ($\text{F}_e\text{SF}_e = 99.8^\circ$) < $\text{CH}_2=\text{SF}_4$ ($\text{F}_e\text{SF}_e = 97.0^\circ$).

For $\text{X}=\text{SF}_4$ compounds, the temperature dependence of the NMR spectra also correlates with the F_eSF_e bond angle; i.e., for large equatorial angles we observe small barriers to pseudorotation and vice versa. For $\text{O}=\text{SF}_4$ ($\text{F}_e\text{SF}_e = 114.9^\circ$) pseudorotation occurs even at -150 °C; i.e., the barrier to pseudorotation is smaller than 5 kcal/mol, while in $\text{CH}_3\text{N}=\text{SF}_4$ ($\text{F}_e\text{SF}_e = 102.6^\circ$) and coalescence temperature \sim -30 °C it is estimated in the order of 10 kcal/mol. In $\text{FN}=\text{SF}_4$ ($\text{F}_e\text{SF}_e = 99.8^\circ$) at +100 °C only broadening of the F_a signals is observed; in $\text{CH}_2=\text{SF}_4$ ($\text{F}_e\text{SF}_e = 97^\circ$) no change in the NMR spectra is found up to 100 °C (the barrier in the last two molecules should be larger than 20–25 kcal/mol).

Acknowledgment. We are grateful to Professor J. E. Boggs, University of Texas, Austin, TX, for providing the computational facilities for the *ab initio* calculations, to Mr. Machinek, Organisch Chemisches Institut der Universität Göttingen, for recording the ^1H NMR spectra, and to Professor G. V. Röschenthaler and Dr. M. Feigl, Universität Bremen, for recording the ^{19}F NMR spectra. H.O. wishes to express his appreciation to NATO for a travel grant (No. 1565) which made the *ab initio* calculations possible. The authors are grateful to the reviewer for helpful suggestions.

Registry No. $\text{CH}_3\text{N}=\text{SF}_4$, 66901-49-3; $\text{HN}=\text{SF}_4$, 80594-79-2.

Supplementary Material Available: A listing of total electron diffraction intensities for $\text{CH}_3\text{N}=\text{SF}_4$ (2 pages). Ordering information is given on any current masthead page.

- (25) E. L. Muetteries, W. Mahler, and R. Schmutzler, *Inorg. Chem.*, **2**, 613 (1963).
 (26) R. J. Gillespie, “Molecular Geometry”, Van Nostrand-Reinhold, London, 1972.
 (27) M. W. Tolles and W. D. Gwinn, *J. Chem. Phys.*, **36**, 1119 (1962).

- (28) K. Christe and H. Oberhammer, *Inorg. Chem.*, **20**, 296 (1981).